PAPER • OPEN ACCESS

On the use of entangled wire materials in pre-tensioned rocking columns

View the article online for updates and enhancements.

Recent citations

- Numerical investigation of nonlinear static and dynamic behaviour of self-centring rocking segmental bridge piers
Ehsan Ahmadi and Mohammad M. Kashani

IOP ebooks™

Bringing you innovative digital publishing with leading voices to create your essential collection of books in STEM research.

Start exploring the collection - download the first chapter of every title for free.

On the use of entangled wire materials in pre-tensioned rocking columns

E Ahmadi, M M Kashani

University of Southampton, Faculty of Engineering and Physical Sciences, Southampton, SO17 1BJ, UK

E.ahmadi@soton.ac.uk

Abstract. This research explores potential application of entangled wire materials as intermediate layers between segments of pre-tensioned segmental bridge columns. An ensemble of free-decay vibration tests was conducted on small-scale columns with various configurations of intermediate layers. Wooden blocks were used for segments and the entire system was tightened together using a pre-tensioned steel tendon. Damping and frequency of the columns were determined and compared. It is demonstrated that entangled wire materials substantially increase total damping of the entire system in rocking. This result is very encouraging for future application of entangled wire materials in testing large-scale pre-tensioned segmental bridge columns. However, shear and axial stiffness of the layers require further improvement to reduce their large shear and axial deformations.

1. Introduction

Bridges play an important role in transportation systems and any disruption in normal performance of bridges imposes high financial costs after destructive earthquakes. Many bridges, located in highly seismic areas, experience harsh material ageing and deterioration [1]. Bridge piers also crack under lateral deformations of the deck, and this accelerates deterioration in monolithic concrete bridges [2]. Further, bridge piers are designed for high plastic deformations in order to reach high energy dissipation during seismic loadings [3]. However, very large permanent displacements remain in bridge piers leading to non- functional structures after seismic events [4]. Thus, segmental precast structural systems are used with more durable materials in accelerated bridge construction (ABC) [5].

It is demonstrated in the literature that pre-tensioned segmental bridge piers are reliable alternative to the conventional bridge construction [6]. The rocking pier segments not only allow for offsite manufacturing which expedites construction time (i.e. ABC), but also reduce the deformations of the pier under lateral dynamic loading (i.e. seismically resilient). However, the rocking mechanism does not provide adequate damping under seismic loading, and thus energy-dissipating elements are needed be added to the bridge pier [7]. These added elements generate high energy dissipation through their large plastic deformations, and thus need be replaced after seismic events. Further, sever damages to concrete is also produced in contact areas due to high contact stress on the rocking surfaces. More recently, hybrid sliding-rocking joints was added to the pre-tensioned segmental bridge pier [8] to improve their shortcomings, but plastic deformations was still observed. To have a damage free bridge column, a biologically-inspired bridge pier was introduced by Kashani et al. [9],[10]. Intermediate rubber layers

were added between segments of the pre-tensioned column. It was found that the proposed vertebral system provides desired rocking behaviour under dynamic base excitations. However, rubber layers did not generate sufficient energy dissipation. Clearly then, the proposed novel system lacks an efficient material as the intervertebral disks to improve damping level of the system.

On the other hand, entangled wire materials (EWMs – also called metal rubber) are increasingly used in the aerospace industry as dampers in pipes and gas turbine engines, and are also considered as a good shock-absorbent material due to its favourable fatigue life and high damping. These properties make EWMs a potential alternative for use in the biologically-inspired bridge pier as intervertebral disks. Nickel-based EWMs have shown high potential for vibration damping and energy dissipations under dynamic compressive and shear excitations [11]. At low-amplitude vibrations, static friction dominates sliding friction. At large-amplitude vibrations, the loss factor may reduce. Thus, dynamic performance of EWMs under large deformations are investigated in this work for their potential use in the novel biologically-inspired bridge pier.

In summary, although the proof of concept studies on the rocking behaviour of the novel biologically-inspired bridge pier showed promising results, an alternative material to the rubber layers is needed to increase energy dissipation capacity in the system. Therefore, this study addresses this knowledge gap and employs entangled wire materials (EWMs) as an alternative material for use as intervertebral discs. To assess dynamic performance of the system, free-decay vibration tests are conducted on a small-scale simplified vertebral column (with varying EWM arrangements and post-tension force of the tendon) to characterise nonlinear dynamic properties of the system. This work is a preliminary study to lay the scientific foundation for further development of this novel system to be tested at large scales for potential use in engineering practice.

2. Experimental procedure

2.1. Tested columns
The typical small-scale pre-tensioned segmental column tested in this study is shown in figure 1. It consists of a base, a column, a tendon, and a mass on the top. Ten 60 mm square wooden blocks were used to model the *intervertebral bones* and nickel-based EWM layers were used to simulate *intervertebral discs*. A 35 N mass on the top of the column reflected inertial effects of the deck. A 1.5 mm stainless pre-tensioned tendon was passed through the centre of the blocks and EWM layers. The tendon integrates the whole system and provides self-centring capability. The tendon was connected to a load cell by means of a clamp at the top of the column. A bottom clamp was also used to attach the column to the base. The initial pre-tensioning force of the tendon was controlled using an adjustable screw, which was connected to the tendon. The initial post-tension force of the tendon was provided by hanging weights (15-52 kg) on a knot at the bottom clamp and spinning the knot.

$51.5 \times 51.5 \times 5.3$ mm nickel-based EWM layers with porosity, mass, and shear force of 80%, 21.5 gr, and 67 kN were used. The EWM layers are placed between bottom wooden blocks as rocking moments and deformations are higher at the base. Four different EWM layer configurations were used to investigate the effects of EWM layers on the dynamic behaviour of the column: (1) no EWM layers, (2) two EWM layers, (3) four EWM layers, and (4) six EWM layers between wooden blocks (see figure 1). These columns are respectively named as C0, C2, C4, and C6 hereafter where the numbers indicate number of EWM layers.
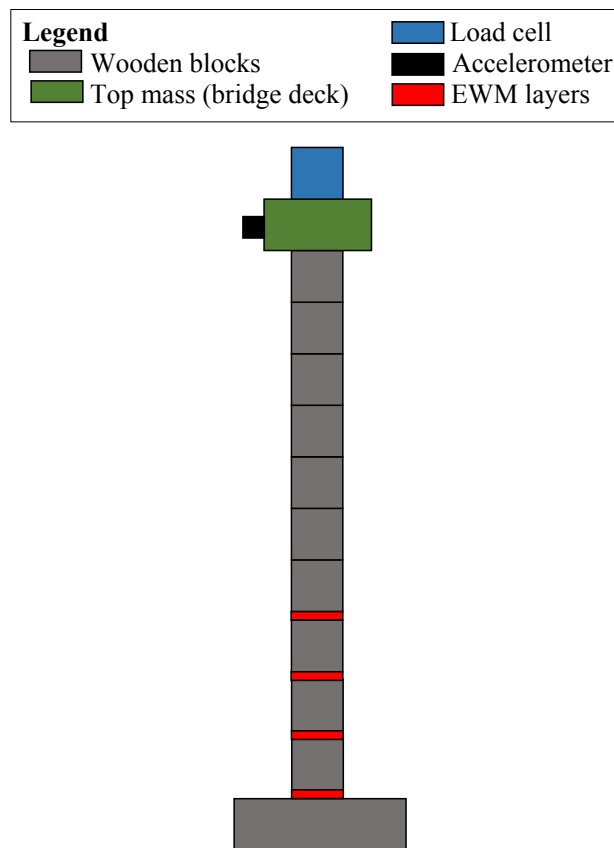
Figure 1. A schematic view of the column used in this study.

2.2. Free-decay vibration experiments

At each free-decay vibration experiment on each of the columns (see figure 1), the tension force of the tendon was adjusted to an initial value, T_i. Then, the top of each column was laterally displaced, and the increment of the tendon force was tracked until a target tension force, T_t, was attained. Finally, the column was allowed to freely vibrate. The acceleration on top of the columns, a_c, was recorded. Two different types of free-decay vibration tests were carried out on the columns: (1) to investigate the effects of target tension force of the tendon on the dynamic behaviour of the column C0, T_i was incrementally increased from 150 N to 300 N by 20 N. For each initial tension force, the target tension force was incrementally increased ten times up to 400 N, and (2) to understand dynamic behaviour of C2, C4, and C6 columns, the initial tension force of the tendon was adjusted to a constant value. The same initial tension force as the maximum for the C0 column, $T_i = 300$ N, was first attempted. The columns remained at where it was displaced. This was because of the deformation of the EWM layers at which the tension force of the tendon reached a stationary state. Thus, the initial tension force of the tendon was increased to 500 N, at which the columns returned to their initial state. The target tension force was varied from 520 N to 600 N by 20 N.

3. Analysis of experimental results

In this section, dynamic characteristics of the columns (i.e. frequency and damping ratio) are determined from free-decay vibration responses for all tests. As the wooden blocks-to-lump mass ratio is very small (≤ 0.0001), the column is modelled with a classical single degree of freedom (SDOF) system as shown in figure 2. The rotational spring shows the rocking stiffness of the columns which changes during the motion due to their geometrically nonlinear behaviour. The equation of motion for the free vibration of the column is thus given by:

$$\ddot{x}_c + 2\xi_c\omega_n\dot{x}_c + \omega_n^2 x_c = 0 \tag{1}$$

where $\ddot{x}_c$, $\dot{x}_c$, and x_c are acceleration, velocity, and displacement of the mass respectively; $\omega_n = 2\pi f_n$ is circular frequency of the column; f_n and ξ_c are natural frequency and damping ratio of the system. Note that equation **Error! Reference source not found.** holds true for both linear and nonlinear systems. For nonlinear systems, natural frequency and damping ratio of the system depend on vibration amplitude and changes between vibration cycles
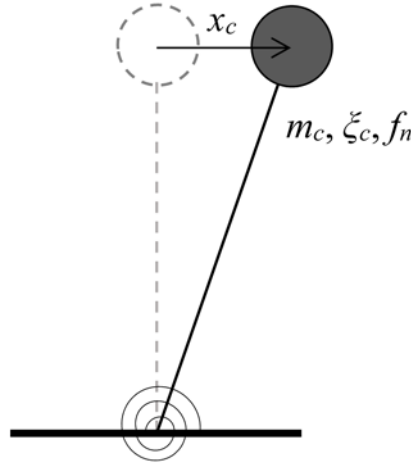

Figure 2. SDOF model of the column.

3.1. Column with no EWM layer
The experimental results of C0 columns exhibited an oscillatory vibration (i.e. underdamped free-decay vibration). For the underdamped column, the amplitudes of the free-decay vibration cycles are determined from [12]:

$$A(t) = A_c e^{-\omega_n\xi_c t} \tag{2}$$

where A_c is the free-decay vibration amplitude at a specific time instant. Figure 3 shows instantaneous frequency, f_n, damping, ξ_c, and amplitude, A_c, for the exemplar C0 column. As seen in figures 3b and 3c, both frequency and damping ratio of the column increase with time. At high vibration amplitudes (4.5 m/s^2 for the exemplar C0 column, see figure 3d), the column's frequency is 2.7 Hz, and the damping ratio is relatively light, 0.0125. Thus, the free-decay vibration results are used to estimate backbone curves [13]. The amplitude-dependent frequencies of the column, f_n, is normalised by the column's frequency, f_c, at very small vibration amplitudes, where the column frequency is independent of the initial tension force of the tendon. Therefore, the backbone curve is described in terms of drift ratio versus frequency ratio. Figure 4 shows non-dimensional backbone and damping ratio skeleton data for all C0 column tests with different initial post-tension force and constant target tension force. The column frequency decreases with vibration amplitude which is typical in lightly-damped structures [14]. However, the damping ratio decreases with vibration amplitude for the column while for typical structures, the damping ratio increases for higher vibration amplitudes due to nonlinear damping effects involved. This behaviour comes from the tendon's effects on the integrity of the wooden blocks. At high vibration amplitudes, despite the compression force acting on wooden blocks being larger because of higher tensions in the tendon, the friction damping between blocks are insignificant due to the joint opening and rocking. As the column becomes closer to its stationary position, the wooden blocks contact area increases, and friction damping increases accordingly.
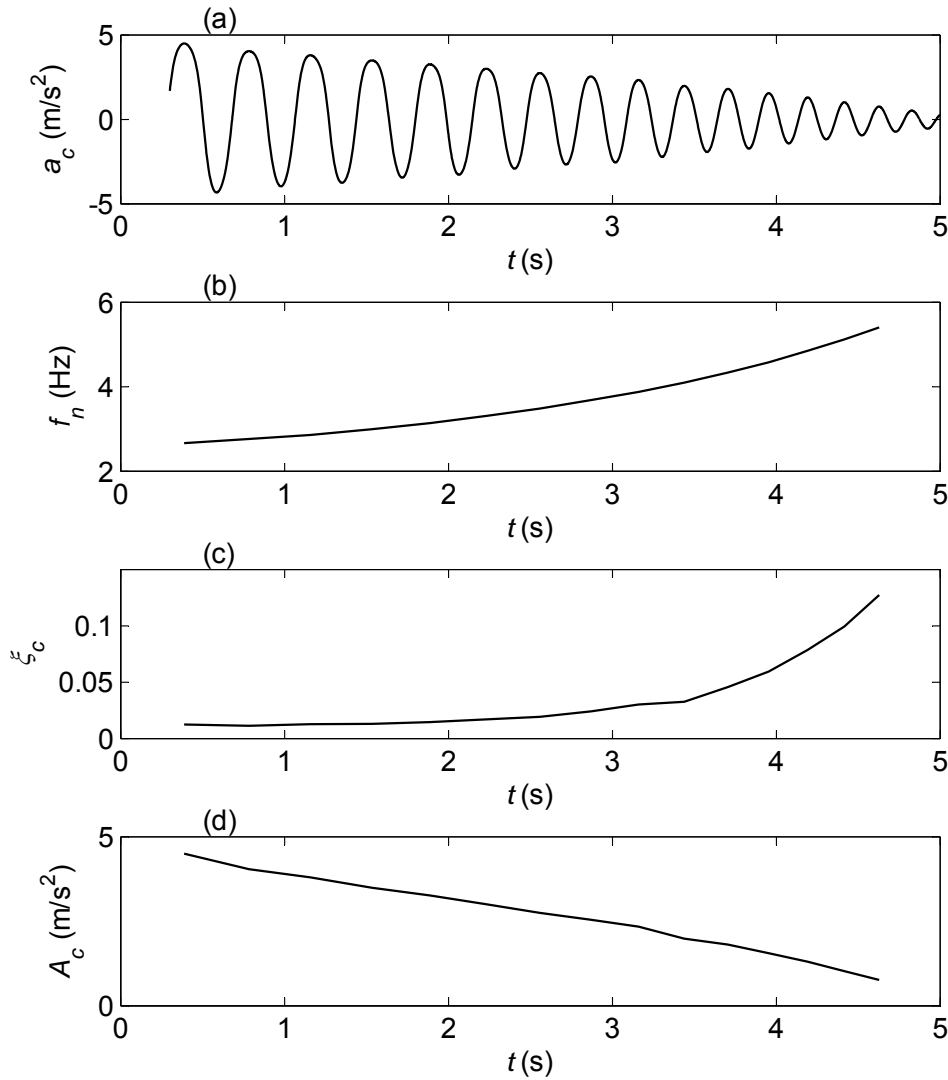
Figure 3. For an exemplar no-EWM layer column test: (a) filtered acceleration response, (b) temporal frequency, (c) temporal damping, and (d) vibration amplitude.

The normalised backbone data follows similar trend independent of initial tension force, and this demonstrates that initial tension force of the tendon does not affect the stiffness of the column (see figure 4a). However, as the initial tension force increases, the damping ratio move towards lower damping ratios (see figure 4b). Figure 5 shows non-dimensional backbone and damping ratio skeleton data for all C0 column tests with different initial tension force and different target tension forces. The results are similar to those with constant target tension force. This demonstrates that no residual deformation remains in the system and the tendon's tension force returns the column to its stationary state through similar force-displacement behaviour.
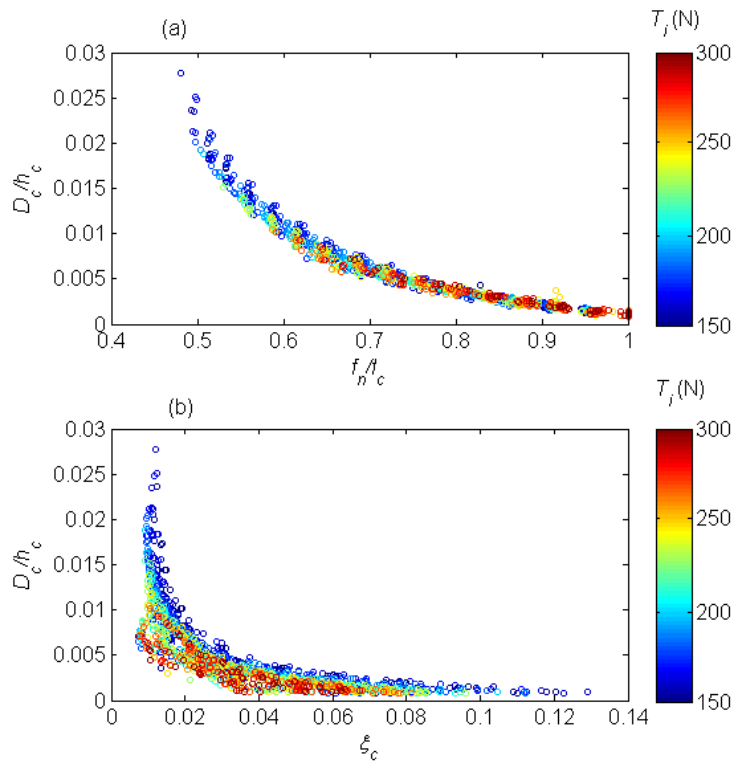
Figure 4. For all C0 column tests with different initial tension force and constant target tension force, T_t = 400 N: (a) backbone estimation data, and (b) damping ratio skeleton data.
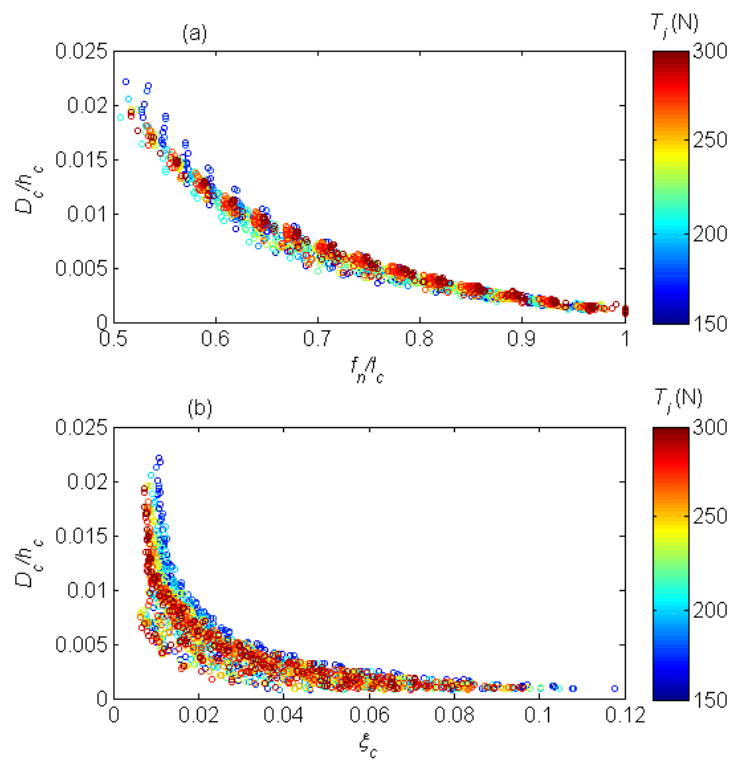

Figure 5. For all C0 column tests with various initial tension and target tension forces: (a) backbone estimation data, and (b) damping ratio skeleton data.

3.2. Columns with EWM layers

The free-decay vibration response of the C2 exemplar tests are very similar to behaviour of overdamped free-decay systems. Thus, as the behaviour is roughly non-oscillatory and the columns moves back into its stationary state after a few vibration cycles, the backbone and skeleton data cannot be obtained for columns with EWM layers. For these overdamped columns, from the auto spectral density (ASD) of the acceleration response, it is concluded that the total response is the sum of two responses: a lower-frequency response, and a higher-frequency response. To determine the lower-frequency component of the response, a low-pass 4th order Butterworth filter was used. Subtracting the lower-frequency response component from the total response, the higher-frequency response component is determined. It is seen that the higher-frequency response component exhibits an oscillatory vibration (see figure 6a) with a few cycles of vibration. Figure 6b shows the frequency of the higher-frequency response component from free-decay method. The higher frequency from the free-decay method at large vibration amplitudes is very close to that obtained from auto spectral density of the column response.
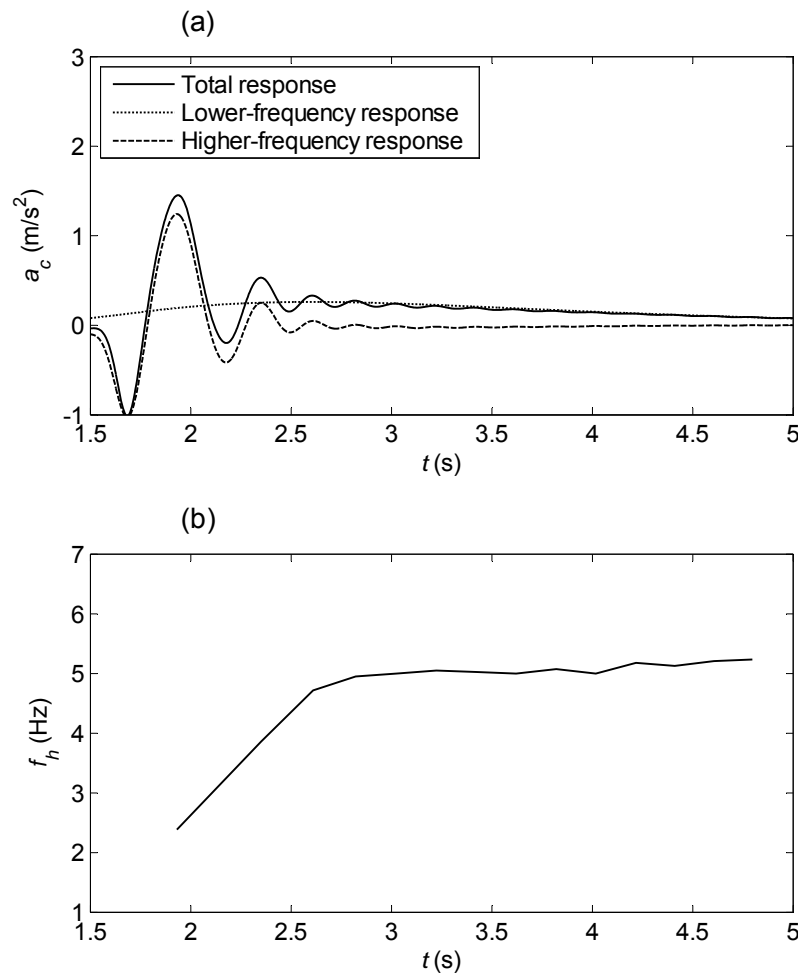

Figure 6. For the exemplar two-EWM layer column test: (a) total acceleration response and its higher- and lower-frequency components, and (b) higher frequency.

Figure 7 shows the natural frequency and damping for all columns with EWM layers versus different target tension forces. The natural frequencies of the columns are much lower compared to the column C0 meaning the columns are more flexible. As the number of layers increases, the natural frequency reduces further (see figure 7a). Also, the damping of columns with EWM layers is far higher than the

column without EWM layers. This shows high energy dissipation of these columns at which vibration goes to zero within a few cycles of vibration. Comparing damping ratios of the columns C2, C4, and C6 show higher capability of the columns with higher EWM layers to dissipate vibration energy as expected.
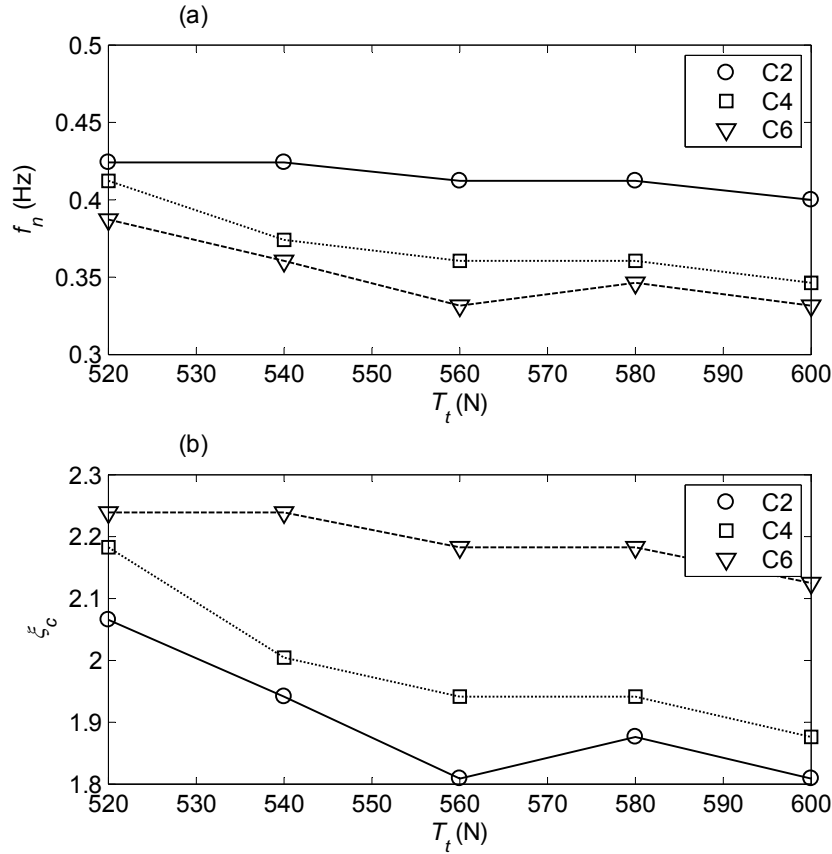

Figure 7. For all columns with EWM layers: (a) natural frequency, and (b) damping ratio versus target tension force.

4. Conclusions

This work addresses the potential use of entangled wire materials in a novel bridge pier inspired from human spine mechanism. To this end, a suit of free-decay vibration experiments were carried out on a small-scale column made from wooden blocks as vertebrae and entangled wire material layers as intervertebral discs, tightened r by a steel tendon. The rocking acceleration at the top of the column was then measured for different configurations of intermediate layers. It is shown that the column without any intermediate layer is an oscillatory underdamped system while using intermediate layers highly increases damping of the column, and an overdamped system is formed. Moreover, it is seen from the free-decay vibration test results that the dynamic stiffness or frequency of columns with the intermediate layers reduces, and the column returns to its initial state within a few cycles of vibration. Even though the energy-dissipation capacity of entangled wire materials was shown to be very beneficial, large shear deformations of the layers led to significant drift ratios. Hence, a material with high energy dissipation capacity and shear stiffness is well suited to be used in pre-tensioned segmental columns as it dampens rocking motion with creating lower drift ratios.

5. Acknowledgment

References

[1]   Kashani MM, Crewe AJ and Alexander NA 2017 Structural capacity assessment of corroded RC bridge piers *Proceedings of the Institution of Civil Engineers - Bridge Engineering* **170**(1): 28–41 doi: 10.1680/jbren.15.00023

[2]   Ni Choine M, Kashani MM, Lowes LN, o'Connor A, Crewe AJ, Alexander NA and Padgett JE 2016 Nonlinear dynamic analysis and seismic fragility assessment of a corrosion damaged integral bridge *International Journal of Structural Integrity* **7**(2): 227–239 doi: 10.1108/IJSI-09-2014-0045

[3]   Jara M, Jara JM and Olmos BA 2013 Seismic energy dissipation and local concentration of damage in bridge bents *Structure and Infrastructure Engineering* **9**(8): 794–805 doi: 10.1080/15732479.2011.615330

[4]   Qinghua AI, Dongsheng W, Hongnan LI 2008 Evaluation of the Seismic Performance of Reinforced Concrete Bridge Columns Based on Plastic Hinge Model *14th World Conference of Earthquake Engineering*: pp 1–8.

[5]   Khan MA 2015 Accelerated Bridge Construction. DOI: 10.1016/B978-0-12-407224-4.00006-X

[6]   Roh H and Reinhorn AM 2010 Hysteretic behavior of precast segmental bridge piers with superelastic shape memory alloy bars *Engineering Structures* **32**(10): 3394–3403 doi: 10.1016/j.engstruct.2010.07.013

[7]   Nikbakht E, Rashid K, Hejazi F and Siti AO 2015 Application of shape memory alloy bars in self-centring precast segmental columns as seismic resistance. *Structure and Infrastructure Engineering* **11**(3): 297–309 doi: 10.1080/15732479.2013.876056

[8]   Sideris P 2015 Nonlinear quasi-static analysis of hybrid sliding-rocking bridge columns subjected to lateral loading *Engineering Structures* **101**: 125–137 doi: 10.1016/j.engstruct.2015.06.053

[9]   Kashani MM and Gonzalez-Buelga A 2017 Nonlinear dynamics of self-centring segmental composite rocking column *Procedia Engineering* **199**: 441–446 doi: 10.1016/j.proeng.2017.09.176

[10]   Kashani MM, Gonzalez-Buelga A, Thayalan RP, Thomas RP, and Alexander NA 2018 Experimental investigation of a novel class of self-centring spinal rocking column *Journal of Sound and Vibration* **437**: 308–324 doi: 10.1016/j.jsv.2018.08.034

[11]   Zhang D, Scarpa F, Ma Y, Hong J and Mahadik Y 2014 Dynamic mechanical behavior of nickel-based superalloy metal rubber *Materials and Design* **56**: 69–77 doi: 10.1016/j.matdes.2013.10.088

[12]   Inman DJ 2017 *Vibration with control* John Wiley & Sons

[13]   Londoño JM, Neild SA, and Cooper JE 2015 Identification of backbone curves of nonlinear systems from resonance decay responses *Journal of Sound and Vibration* **348**: 224–38 doi:10.1016/j.jsv.2015.03.015

[14]   Ahmadi E, Živanović S, Caprani C, Evans N and Heirdapour A 2018 A framework for quantification of human-structure interaction in vertical direction *Journal of Sound and Vibration* **432**: 351-372 doi:10.1016/j.jsv.2018.06.054